frontiers in Energy Research

BRIEF RESEARCH REPORT
published: 31 January 2022
doi: 10.3389/fenrg.2022.802883

The Influence of CO_2 Saturated Brine on Microstructure of Coal: Implications for Carbon Geo-Sequestration

Xiaolong Li[1], Hongyan Yu[1,2], Maxim Lebedev[2], Minghui Lu[3], Yujie Yuan[4], Zhen Yang[1], Wei Cheng[1], Sisi Chen[1], Jie Zhan[5,6], Shuaiwei Ding[1] and Lukman Johnson[7]*

[1]State Key Laboratory of Continental Dynamics, Department of Geology, Northwest University, Xi'an, China, [2]WA School of Mines: Minerals, Energy and Chemical Engineering, Curtin University, Kensington, WA, Australia, [3]Department of Geophysics, PetroChina Exploration and Development Research Institute, Beijing, China, [4]School of Earth Sciences, Yunnan University, Kunming, China, [5]Key Laboratory of Deep-Earth Dynamics of Ministry of Natural Resources, Institute of Geology, Chinese Academy of Geological Sciences, Beijing, China, [6]School of Petroleum Engineering, Xi'an Shiyou University, Xi'an, China, [7]Department of Applied Geology, West Australian School of Mines, Curtin University, Kensington, WA, Australia

OPEN ACCESS

Edited by:
Ah-Hyung Alissa Park, Columbia University, United States

Reviewed by:
Yingfang Zhou, University of Aberdeen, United Kingdom
Huaimin Dong, Chang'an University, China
Jianchao Cai, China University of Petroleum, Beijing, China

***Correspondence:**
Hongyan Yu
amelia-yu@hotmail.com

Specialty section:
This article was submitted to Carbon Capture, Utilization and Storage, a section of the journal Frontiers in Energy Research

Received: *27 October 2021*
Accepted: *05 January 2022*
Published: *31 January 2022*

Citation:
Li X, Yu H, Lebedev M, Lu M, Yuan Y, Yang Z, Cheng W, Chen S, Zhan J, Ding S and Johnson L (2022) The Influence of CO_2 Saturated Brine on Microstructure of Coal: Implications for Carbon Geo-Sequestration. Front. Energy Res. 10:802883. doi: 10.3389/fenrg.2022.802883

Carbon dioxide geological storage in deep underground oil and gas reservoirs or coal seam is considered a key technology to effectively mitigate carbon emissions. Deep coal seams are the potential host rock for CO_2 storage, with chemical reactions occurring when coal is exposed to CO_2-saturated brine. However, limited studies have been conducted to reveal the effect of chemical reaction, particularly to unveil how this importantly affects the coal seam porosity at the micrometer scale. In this study, the CO_2 geological storage is simulated using a high-temperature and high-pressure reactor containing CO_2-saturated brine and coal samples. The samples in the previous study on the effect of CO_2 on coal mostly contained high content of carbonate minerals and sulfide minerals. However, the tested Collie coal samples, which are characterized by high content of kaolinite and siderite, are rarely used. This coal was quantitatively analyzed using a scanning electron microscope before and after reaction. The results show that the microstructure of coal matrix was largely changed due to acid exposure. Kaolinite and siderite in the coal matrix were dissolved, the size and morphology of the cleats increased, and the absolute effective porosity also increased significantly. Most importantly, the connectivity of cleat network was improved, leading to an increase in CO_2 storage space and coal seam permeability. Therefore, it is concluded that the microstructure changes of coal can be measured on a microscopic scale, and it is better to be quantitatively evaluated to improve the accuracy and reliability of CO_2 storage in deep coal seams.

Keywords: CO_2 geological storage, coal seam, SEM, CO_2-saturated brine, cleat structure

1 INTRODUCTION

CO_2 storage in deep geological formation is a vital technology that effectively resolves climate change caused by carbon emissions (White et al., 2005; Alemu et al., 2011; Zhou et al., 2017). The main storage places are underground geological reservoirs including deep undeveloped coal seams, deep brine aquifers, and oil and gas reservoirs (Bachu et al., 1994). Solubility trapping is one of the safest

and effective trapping mechanisms (Akhondzadeh et al., 2020; Al-Khdheeawi et al., 2016; Iglauer et al., 2015; Iglauer and Al-Yaseri, 2021; Mitchell et al., 2010; Niu et al., 2015; Zhang et al., 2017) by dissolving CO_2 in the formation water. The density of CO_2-saturated brine (also called live brine) is greater than that of the original formation water; thus, it sinks to the bottom of the reservoir. However, this CO_2-saturated brine in the formation has a pH value of only 3–4, which is strongly acidic that will chemically react with coal seam (Deng et al., 2015; Liu et al., 2018; Menke et al., 2017).

The chemical reaction of coal and CO_2 has been extensively studied in the context of acid stimulation. Such reactions lead to the opening and interconnection of the cleats (Dawson et al., 2015; Hedges et al., 2007). Calcite, dolomite, and magnesite dissolved in the CO_2-saturated brine, causing the opening of originally closed or semi-closed pores, and eventually improved porosity and permeability (Du et al., 2018; Liu et al., 2010). The dissolution of minerals filled in pores and cracks changed the mechanical properties of coal (Anggara et al., 2013; Faiz et al., 2007). However, quantitative micro-pore scale study is limited, which needs to be supplemented to improve the accuracy and safety of CO_2 storage in deep coal seams.

It is although significant to investigate the crucial influence of microstructure changes on the porosity and permeability of coal, current research mainly focuses on the qualitative description of geochemical changes (element migration and mineral changes) (Bertier et al., 2006; Credoz et al., 2011; Farquhar et al., 2015; Gunter et al., 1993; Hedges et al., 2007). SEM has been widely used to study the evolution rules of coal cleats and to capture the cleat geometry in coal (Zhang et al., 2016; Zhang et al., 2017). Yu et al. (2018a) observed the coal cleat morphology through SEM and presented the effect on nanoscale mechanical heterogeneity. Liu et al. (2017) described pore connectivity and types of pores in high-rank coals.

Here, we thus used the reactor to simulate the reaction of CO_2 with the coal seam at high temperature and high pressure. Scanning electron microscopy (SEM) and energy dispersive spectroscopy (EDS) are used to identify and image the changes of specific minerals and the microstructure before and after the reaction and then to evaluate the influence of CO_2-saturated brine on coal microstructure.

2 MATERIALS AND METHODS

2.1 Geological Setting

The Collie Basin located 150 km southeast of Perth is composed of three sub-basins (Cardiff, Shotts, and Muja), covering an area of approximately 230 km^2. It is one of the largest basins in Western Australia. The Permian strata were preserved in a northwest-trending graben (Hocking et al., 1994; Li et al., 2014). The Collie coal seam developed in the Permian throughout the basin (Backhouse, 1991; Yu et al., 2018a), which consisted of three sets of coal seams that were typical carbonaceous coal seams, whose rank was subbituminous and vitrinite reflectance was 0.41–0.61%. The total thickness of Collie coal seams is around 800 m.

2.2 Experimental Procedure

2.2.1 Experimental Materials

Three samples of the Collie formation in the Collie Basin named S1, S2, and S3 were collected to conduct a high-pressure and high-temperature (HPHT) geochemical simulation experiment. The samples are polished by p1200 silicon carbide (particle size is 9.8 ± 0.5 μm) to ensure that the sample is sufficiently smooth for SEM experiments. We injected CO_2 into deionized water that dissolved 5 wt% NaCl to get the CO_2-saturated brine (live brine).

2.2.2 Geochemical Simulation Experiment

We use the experimental instrument to carry out the HPHT geochemical simulation experiment, the volume of the experimental container is 1 L, and the experimental temperature and pressure are 50°C and 20 MPa, respectively. The experimental conditions are calculated from the geothermal gradient of the Collie Basin and the depth of the Collie coal seams. The geochemical simulation experiment was conducted as follows:

1. The samples were polished and imaged by SEM at room temperature and pressure.
2. The sample placed in a reactor and the system was vacuumed for 24 h to ensure no air remained.
3. CO_2 and brine were pressurized to 50°C and 20 MPa and then injected into the reactor. In order to ensure the stability of the reaction system, the temperature and pressure were continuously monitored during the experiment.
4. The sample was took out and put in a vacuum-drying oven after 24 h, and then the SEM experiment was performed.

2.3 SEM Image Processing

Scanning electron microscopy (SEM) was performed to scan the coal samples in different scales (200X–4000X) to investigate the morphological characteristics and mineral element composition of the coal sample. In addition, the energy dispersive spectroscopy (EDS) (Acquafredda et al., 1999) method was performed to get elemental composition, which thus applies to mineral identification and distribution. *Avizo* is used for SEM grayscale image processing. SEM grayscale images were first denoised with a *Gaussian filter* to obtain clearer and more detailed images (Blinchikoff and Zverev, 1976; Mayer et al., 2003; Yu et al., 2018b; Yu et al., 2019a; Yu et al., 2019b) and then segmented by *Watershed Segmentation* module, which can extract the microscopic cleats of the sample from the sample skeleton (Vincent and Soille, 1991; Szeliski, 2010; Zhang et al., 2020). Finally, we used the *Label Analysis* module to quantitatively obtain the sample porosity, equivalent diameter, perimeter, and area before and after solid–liquid reaction. The equivalent diameter refers to the diameter of a circle that is the same as the area occupied by the cleat and represents the size of the cleat. The area fraction refers to the ratio of the number of pixels occupied by cleats to the number of pixels in the overall picture and represents the cleat porosity of the sample.

2.4 X-Ray Diffraction Measurements

XRD experimental analysis was conducted with a Bruker-AXS D8 Advance diffractometer (Yuan et al., 2021). These cleated samples

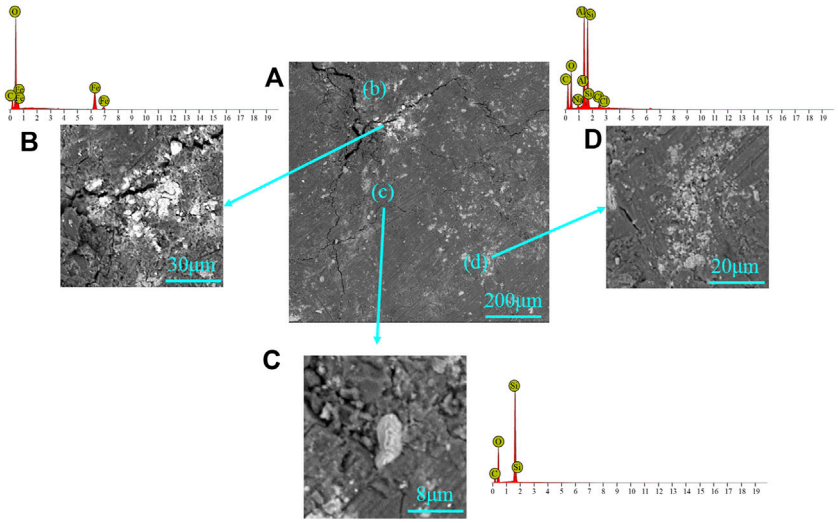

FIGURE 1 | SEM-EDS for the mineral in the coal sample: **(A)** coal matrix, **(B)** siderite, **(C)** quartz, and **(D)** kaolinite.

were ground to 800-mesh and put into a container. Then, the element energy spectrum of the sample was acquired by XRD equipment, compared with the existing standard mineral energy spectrum to determine the mineral type and content.

3 RESULTS AND DISCUSSION

3.1 Mineral Composition and Microstructure

The mineral composition of the coal sample is mainly obtained from the XRD experiment (Yu et al., 2018a). There are three inorganic minerals (not including the coal matrix) in the Collie coal sample: kaolinite (49.1%), quartz (36.6%), and siderite (14.3%). Kaolinite [Al_4 $(Si_4O_{10})(OH)_8$] is a common aluminosilicate mineral in sedimentary rocks, while siderite ($FeCO_3$) is the carbonate mineral. These two minerals can dissolve in acidic solutions, which in total take more than 60% of the mineral composition.

The microstructure of the coal sample was imaged by SEM. The SEM images showed the coal consisted of minerals and coal matrix. The coal matrix is very dense with almost no pores, and cleats can be clearly observed with width 0.1–1 μm. The minerals in the SEM images show different brightness. The brighter area represented high-density minerals, and the dark parts were lower density minerals. EDS can obtain elemental composition, combining with SEM images to identify mineral types. SEM-EDS results indicated that panel (B) in **Figure 1** is siderite, as the EDS results showed the main elements in this mineral are iron, carbon, and oxygen, while the minerals are granular and gelatinous. Hence, panels (C) and (D) are quartz (silicon and oxygen) and kaolinite (aluminosilicate minerals and kaolinite booklets), respectively. These cleats provided a flow channel for live brine and increased the reaction area when the sample had contact with the acid system.

3.2 Microstructural Change

SEM images were obtained in different scale and resolution before and after the experiment (**Figure 2**). Rows (A) and (B) are the sample images before the experiment, whereas rows (C) and (D) are the results after the reaction. Among them, rows (A) and (D) are in low resolution for the large view of the sample, while rows (B) and (C) are in high resolution for accurate image processing.

It can be seen that there are rarely matrix pores in the sample; however, there are many cleats throughout the sample. These cleats provided a flow channel for live brine and increased the reaction area when the sample had contact with the acid system. The morphology and size of the cleats in the coal sample critically changed. Some cleats enlarged and some closed, and also new cleats were generated after the reaction (**Figure 3**). This phenomenon may be generated by mineral dissolution and small piece migration. The pH of CO_2 saturated brine is very low at high temperature and high pressure, leading to mineral dissolution (Du et al., 2019).

We extracted the cleats from SEM images, shown in column (2) of **Figure 3**. The expansion, generation, and closure of the cleats are obviously shown. We found that most of the cleats especially primary cleats enlarged a lot in these three samples, while the disconnected narrow cleats expanded visibly after the reaction (points c and d, e and f, k and l), forming large cleats. Moreover, new cleats were generated (points g and h, i and j). However, the cleats (point a) in S1 significantly shrunk (point b) after the reaction. The dissolution of siderite and kaolinite is the main reason leading to cleat expansion and new cleat generation (He and Morse, 1993; O'Connor et al., 2000; Kanakiya et al., 2017). However, mineral dissolution resulted in the small pieces in the coal sample migration, in turn causing some cleats shrink or even disappear. These changes in the microstructure illustrate that the disappearance of small individual cleats makes the cleat network better connected.

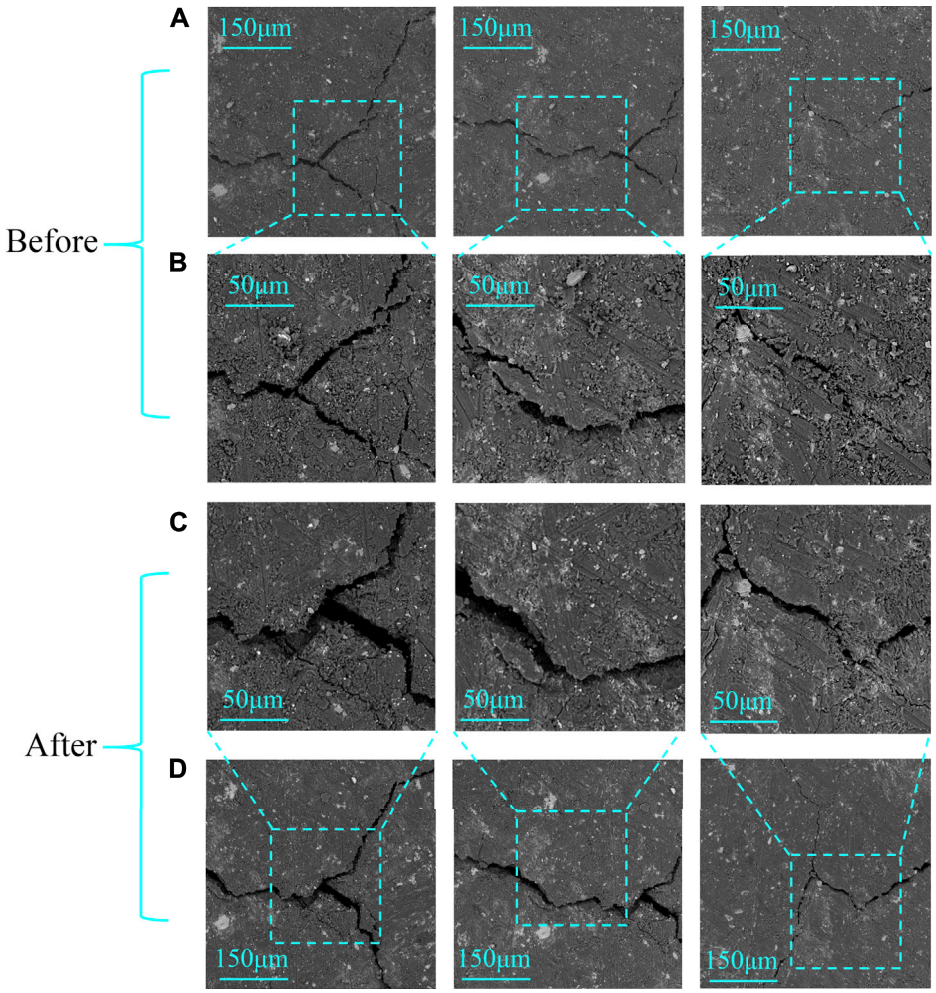

FIGURE 2 | SEM images before **(A,B)** and after **(C,D)** the reaction; rows **(B,C)** are in high resolution, while rows **(A,D)** are in low resolution.

Both the dissolution and migration of minerals affect the microstructure of the coal sample. The SEM images showed that the cleat area has increased significantly, indicating that the porosity and pore volume of the coal sample have increased after the experiment, which is consistent with that reported in the previous research (Liu et al., 2015; Liu et al., 2017; Yu et al., 2018a; Zhang et al., 2016). It can also be observed that the original small cleats were connected forming a new large path, and such a change will greatly increase permeability (Cai et al., 2018).

3.3 Cleat Quantified Analysis

We processed the image and calculated the specific cleat change. All cleats were identified and marked with a different color, and the largest cleats (max-cleat) of each sample were also extracted (**Figure 3**). The tested samples were analyzed using the average cleat aspect ratio, cleat porosity, average cleat width, and cleat density. Meanwhile, the perimeter, area, aspect ratio, and fraction were applied for the maximum cleat. The results showed that the cleats in the coal sample after geochemical reaction dramatically changed, especially the largest micro-cleats (**Figure 4**).

The cleat porosity of these three samples all rose before and after the reaction, changing from 3.36 to 10.33%. The average cleat width also increased after the reaction, and the variation was from 0.29 to 5.49. Such results indicated CO_2-saturated brine can indeed expand the cleats. The average aspect ratio varied in each cleat, from 6.27 to 21.78. The average aspect ratio of S1 decreased, while that of S2 and S3 increased after the reaction. The main reason that can explain this is many isolated cleats were connected after the reaction in S2 and S3, therefore leading to the rise in the average aspect ratio. The cleat density shows a distinct change, due to some smaller cleats merging into larger cleats and the formation of new cleats.

The max-cleat of each sample is significantly important for fluid and gas flooding; hence, we also analyzed the max-cleat (**Figure 4**). The size max-cleat also increased after the reaction: the largest increment value is 127.83% (max-cleat perimeter), 308.02% (max-cleat area), 31.27 (max-cleat aspect ratio), and 49.19% (max-cleat area faction). It is concluded that the max-cleat changed mostly among all cleats, which would severely put an impact on the sample permeability.

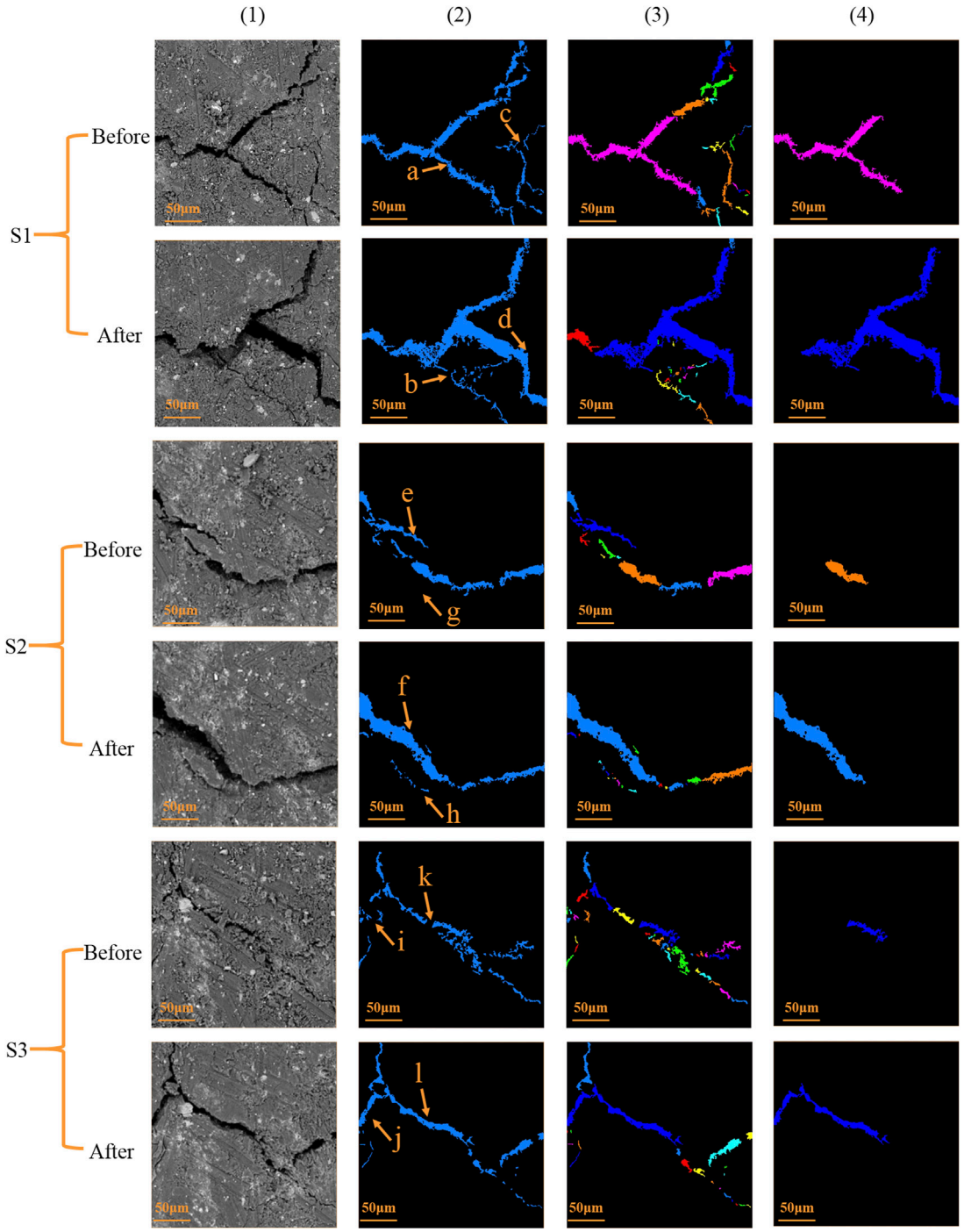

FIGURE 3 | Comparison of cleat shape and size before and after the reaction: (1) the original SEM image, (2) extracted cleat, (3) individual cleats, and (4) extracted largest cleat.

The increment of cleat size after the reaction illustrated that the micro-cleat structure in the coal has greatly changed, leading to the increase of porosity and the connectivity improvement of the cleat network, thereby providing a better flooding path and storage space for CO_2 in the deep coal seam. It is worth mentioning that this result is consistent with that reported by Zhang et al. (2018), who observed that the calcite-rich coal was partially dissolved during CO_2-saturated brine flooding, resulting in a significant increase in absolute porosity and connectivity. Yu et al. (2018b) studied fractured shale exposed to CO_2-saturated brine, and they also found that connectivity and apertures of micro-fractures in the shale were significantly improved after

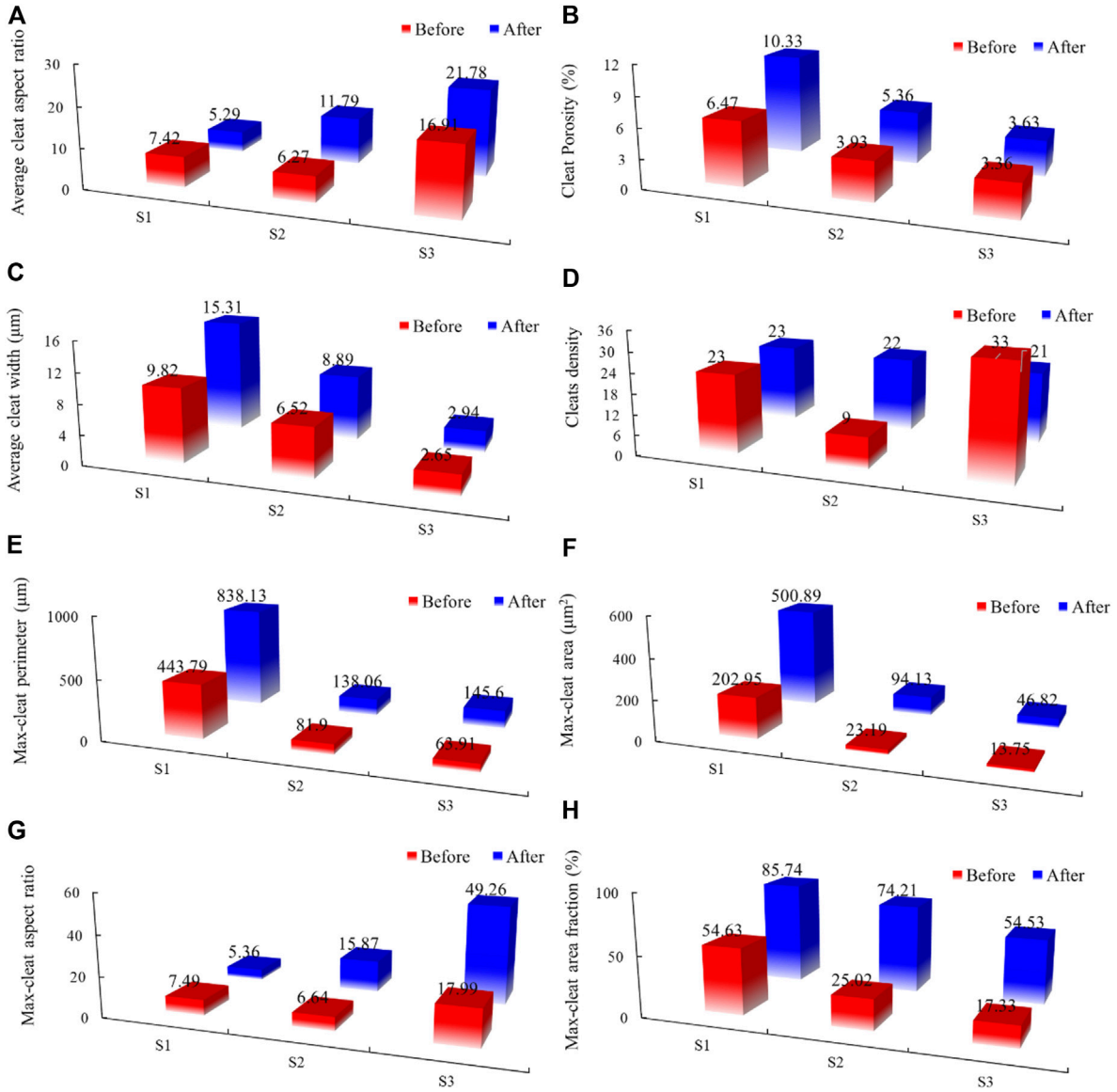

FIGURE 4 | Histogram of the variation of cleat parameters in coal: **(A)** total aspect ratio; **(B)** porosity; **(C)** average width of all cleats; **(D)** fracture density; **(E)** perimeter; **(F)** area; **(G)** aspect ratio of maximum cleat; **(H)** the maximum cleat fraction.

CO_2-saturated brine injection. However, CO_2-saturated brine did not always increase rock permeability. The permeability of unconsolidated sandstone was greatly reduced after CO_2-saturated brine injection. The decrease in permeability was induced by the blockage of pore throats, caused by the release, migration, and reattachment of fine particles at the initial stage of CO_2 injection (Yu et al., 2019a). Nevertheless, the storage of CO_2 in different formations still needs further research.

4 CONCLUSION

CO_2 injection into deep geological formations has been proven to be an effective way to mitigate climate change. However, the injected CO_2 reacts with the formation water and forms acidic brine (Yu et al., 2018c; Yu et al., 2019a), which would react with the coal seam and change the microstructure of the coal seam. Therefore, it is very important to fully understand the interaction of CO_2-saturated brine with coal seam and its impact on the microstructure. However, most of the work is focused on the qualitative geochemical changes (Du et al., 2019; Gunter et al., 1993; Hedges et al., 2007), and there is only limited work to better understand micron-scale dissolution, although microscale microstructure changes are critical to the CO_2 storage in deep coal seams.

Therefore, we conducted experiments to study microstructure changes before and after reaction between CO_2-saturated brine and coal samples at the micrometer scale. The microstructure of coal partially dissolves after being exposed to live brine, which is

consistent with the change in cleat size and shape. The mineral dissolution at the edge of the cleat greatly increases the volume fraction of the cleat, resulting in a significant increase in the equivalent diameter and area of the cleat. In addition, it is important that the reaction between live brine and coal causes a better connectivity of the cleat network because the fraction of the maximum cleat has increased from 25 to 72.4%, which means that some isolated cleats connected increased the fraction of the maximum cleat, leading to an increase in CO_2 storage space and coal seam permeability.

Thus, overall, we have concluded that the changes in the microstructure of coal should be measured on a microscale, preferably combined with quantitative analysis, to improve the accuracy and reliability of CO_2 storage in deep coal seams.

DATA AVAILABILITY STATEMENT

The original contributions presented in the study are included in the article/Supplementary Material, and further inquiries can be directed to the corresponding author.

AUTHOR CONTRIBUTIONS

XL was mainly responsible for analyzing and displaying research data, especially visualization data display, as well as performing research on published works and writing drafts. MAL conducted experiments and data collection, monitored the overall experimental process, and proofread the experimental data. MIL and JZ provided the experimental samples and materials needed for the research. ZY conducted a preliminary review of the draft, proposed some suggestions for revision, and participated in subsequent revisions. WC and SC were responsible for making some histograms and looking up references cited in the text. HY proposed the idea and the design of the overall draft, checked the experimental results, and conducted a final critical review and comment on the draft with. During the second revision, YY and LUJ made changes to the grammar and vocabulary of the text, SD made changes to the figures.

FUNDING

This work was jointly funded by the National Natural Science Foundation of China (No. 41902145), Natural Science Basic Research Plan in Shaanxi Province of China (No. 2020JQ-594), Young Researcher of Science and Technology and Foreign Expert Service Plan in Shaanxi Province (Nos. 2021KJXX-28 and 2021JZY-016), and State Key Laboratory of Continental Dynamics at Northwest University in China. This work was also supported by the Youth Project of National Natural Science Foundation of China (Grant No. 52004219), the Scientific Research Program Funded by Shaanxi Provincial Education Department (Grant No. 20JS117), the Natural Science Basic Research Program of Shaanxi (Grant No. 2020JQ-781), and the Pawsey Supercomputing Centre, who provided the Avizo 9.5 image processing software and workstation, with funding from the Australian Government and the Government of Western Australia.

REFERENCES

Acquafredda, P., Andriani, T., Lorenzoni, S., and Zanettin, E. (1999). Chemical Characterization of Obsidians from Different Mediterranean Sources by Non-destructive SEM-EDS Analytical Method. *J. Archaeological Sci.* 26, 315–325. doi:10.1006/jasc.1998.0372

Akhondzadeh, H., Keshavarz, A., Al-Yaseri, A. Z., Ali, M., Awan, F. U. R., Wang, X., et al. (2020). Pore-scale Analysis of Coal Cleat Network Evolution through Liquid Nitrogen Treatment: A Micro-computed Tomography Investigation. *Int. J. Coal Geology.* 219, 103370. doi:10.1016/j.coal.2019.103370

Al-Khdheeawi, E. A., Vialle, S., Barifcani, A., Sarmadivaleh, M., and Iglauer, S. (2016). Influence of CO_2-wettability on CO_2 Migration and Trapping Capacity in Deep saline Aquifers. *Greenhouse Gases: Sci. Tech.* 7 (2), 328–338. doi:10.1002/ghg.1648

Alemu, B. L., Aagaard, P., Munz, I. A., and Skurtveit, E. (2011). Caprock Interaction with CO2: A Laboratory Study of Reactivity of Shale with Supercritical CO2 and Brine. *Appl. Geochem.* 26, 1975–1989. doi:10.1016/j.apgeochem.2011.06.028

Anggara, F., Sasaki, K., and Sugai, Y. (2013). Mineral Dissolution/Precipitation during CO2 Injection into Coal Reservoir: A Laboratory Study. *Energ. Proced.* 37, 6722–6729. doi:10.1016/j.egypro.2013.06.605

Bachu, S., Gunter, W. D., and Perkins, E. H. (1994). Aquifer Disposal of CO2: Hydrodynamic and mineral Trapping. *Energ. Convers. Manag.* 35, 269–279. doi:10.1016/0196-8904(94)90060-4

Backhouse, J. (1991). Permian Palynostratigraphy of the Collie Basin, Western Australia. *Rev. Palaeobotany Palynology* 67, 237–314. doi:10.1016/0034-6667(91)90046-6

Bertier, P., Swennen, R., Laenen, B., Lagrou, D., and Dreesen, R. (2006). Experimental Identification of CO_2–water–rock Interactions Caused by Sequestration of CO_2 in Westphalian and Buntsandstein Sandstones of the Campine Basin (NE-Belgium). *J. geochemical exploration* 89 (1-3), 10–14. doi:10.1016/j.gexplo.2005.11.005

Blinchikoff, H. J., and Zverev, A. I. (1976). *Filtering in the Time and Frequency Domains*. New York, NY: John Wiley & Sons.

Cai, J., Lin, D., Singh, H., Wei, W., and Zhou, S. (2018). Shale Gas Transport Model in 3D Fractal Porous media with Variable Pore Sizes. *Mar. Pet. Geology.* 98, 437–447. doi:10.1016/j.marpetgeo.2018.08.040

Credoz, A., Bildstein, O., Jullien, M., Raynal, J., Trotignon, L., and Pokrovsky, O. (2011). Mixed-layer Illite-Smectite Reactivity in Acidified Solutions: Implications for Clayey Caprock Stability in CO2 Geological Storage. *Appl. Clay Sci.* 53, 402–408. doi:10.1016/j.clay.2011.01.020

Dawson, G. K. W., Pearce, J. K., Biddle, D., and Golding, S. D. (2015). Experimental mineral Dissolution in Berea Sandstone Reacted with CO 2 or SO 2 -CO 2 in NaCl Brine under CO 2 Sequestration Conditions. *Chem. Geology.* 399, 87–97. doi:10.1016/j.chemgeo.2014.10.005

Deng, H., Fitts, J. P., Crandall, D., McIntyre, D., and Peters, C. A. (2015). Alterations of Fractures in Carbonate Rocks by CO2-Acidified Brines. *Environ. Sci. Technol.* 49 (16), 10226–10234. doi:10.1021/acs.est.5b01980

Du, Y., Sang, S., Wang, W., Liu, S., Wang, T., and Fang, H. (2018). Experimental Study of the Reactions of Supercritical CO2 and Minerals in High-Rank Coal under Formation Conditions. *Energy Fuels* 32 (2), 1115–1125. doi:10.1021/acs.energyfuels.7b02650

Du, Y., Sang, S., Pan, Z., Wang, W., Liu, S., Fu, C., et al. (2019). Experimental Study of Supercritical CO2-H2O-coal Interactions and the Effect on Coal Permeability. *Fuel* 253, 369–382. doi:10.1016/j.fuel.2019.04.161

Faiz, M. M., Saghafi, A., Barclay, S. A., Stalker, L., Sherwood, N. R., Whitford, D. J., et al. (2007). Evaluating Geological Sequestration of CO2 in Bituminous Coals: The Southern Sydney Basin, Australia as a Natural Analogue. *Int. J. greenhouse gas Control* 1 (2), 223–235. doi:10.1016/s1750-5836(07)00026-6

Farquhar, S. M., Pearce, J. K., Dawson, G. K. W., Golab, A., Sommacal, S., Kirste, D., et al. (2015). A Fresh Approach to Investigating CO 2 Storage: Experimental CO 2 -Water-Rock Interactions in a Low-Salinity Reservoir System. *Chem. Geology.* 399, 98–122. doi:10.1016/j.chemgeo.2014.10.006

Gunter, W. D., Perkins, E. H., and McCann, T. J. (1993). Aquifer Disposal of CO2-rich Gases: Reaction Design for Added Capacity. *Energ. Convers. Manag.* 34 (9-11), 941–948. doi:10.1016/0196-8904(93)90040-h

He, S., and Morse, J. W. (1993). The Carbonic Acid System and Calcite Solubility in Aqueous Na-K-Ca-Mg-Cl-SO4 Solutions from 0 to 90°C. *Geochimica et Cosmochimica Acta* 57, 3533–3554. doi:10.1016/0016-7037(93)90137-l

Hedges, S. W., Soong, Y., Jones, J. R. M., Harrison, D. K., Irdi, G. A., Frommell, E. A., et al. (2007). Exploratory Study of Some Potential Environmental Impacts of CO2 Sequestration in Unmineable Coal Seams. *Int. J. Environ. Pollut.* 29, 457–473. doi:10.1504/ijep.2007.014232

Hocking, R., Mory, A., and Williams, I. 1994. An Atlas of Neoproterozoic and Phanerozoic Basins of Western Australia. In The sedimentary basins of western australia: Proceedings of petroleum exploration society of australia symposium, perth, August 1994, 21–43.

Iglauer, S., and Al-Yaseri, A. (2021). Improving basalt Wettability to De-risk CO2 Geo-Storage in Basaltic Formations. *Adv. Geo-energy Res.* 5 (3), 347–350. doi:10.46690/ager.2021.03.09

Iglauer, S., Al-Yaseri, A. Z., Rezaee, R., and Lebedev, M. (2015). CO2 Wettability of Caprocks: Implications for Structural Storage Capacity and Containment Security. *Geophys. Res. Lett.* 42 (21), 9279–9284. doi:10.1002/2015gl065787

Kanakiya, S., Adam, L., Esteban, L., Rowe, M. C., and Shane, P. (2017). Dissolution and Secondary mineral Precipitation in Basalts Due to Reactions with Carbonic Acid. *J. Geophys. Res. Solid Earth* 122, 4312–4327. doi:10.1002/2017jb014019

Li, T., Zhang, L., Dong, L., and Li, C.-Z. (2014). Effects of Gasification Atmosphere and Temperature on Char Structural Evolution during the Gasification of Collie Sub-bituminous Coal. *Fuel* 117, 1190–1195. doi:10.1016/j.fuel.2013.08.040

Liu, C. J., Wang, G. X., Sang, S. X., and Rudolph, V. (2010). Changes in Pore Structure of Anthracite Coal Associated with CO2 Sequestration Process. *Fuel* 89 (10), 2665–2672. doi:10.1016/j.fuel.2010.03.032

Liu, C. J., Wang, G. X., Sang, S. X., Gilani, W., and Rudolph, V. (2015). Fractal Analysis in Pore Structure of Coal under Conditions of CO 2 Sequestration Process. *Fuel* 139, 125–132. doi:10.1016/j.fuel.2014.08.035

Liu, S., Sang, S., Wang, G., Ma, J., Wang, X., Wang, W., et al. (2017). FIB-SEM and X-ray CT Characterization of Interconnected Pores in High-Rank Coal Formed from Regional Metamorphism. *J. Pet. Sci. Eng.* 148, 21–31. doi:10.1016/j.petrol.2016.10.006

Liu, B., Fu, X., and Li, Z. (2018). Impacts of CO2-brine-rock Interaction on Sealing Efficiency of Sand Caprock: A Case Study of Shihezi Formation in Ordos basin. *Adv. Geo-energy Res.* 2 (4), 380–392. doi:10.26804/ager.2018.04.03

Mayer, M., Kriebel, J. K., Tosteson, M. T., and Whitesides, G. M. (2003). Microfabricated Teflon Membranes for Low-Noise Recordings of Ion Channels in Planar Lipid Bilayers. *Biophysical J.* 85, 2684–2695. doi:10.1016/s0006-3495(03)74691-8

Menke, H. P., Bijeljic, B., and Blunt, M. J. (2017). Dynamic Reservoir-Condition Microtomography of Reactive Transport in Complex Carbonates: Effect of Initial Pore Structure and Initial Brine pH. *Geochimica et Cosmochimica Acta* 204, 267–285. doi:10.1016/j.gca.2017.01.053

Mitchell, A. C., Dideriksen, K., Spangler, L. H., Cunningham, A. B., and Gerlach, R. (2010). Microbially Enhanced Carbon Capture and Storage by mineral-trapping and Solubility-Trapping. *Environ. Sci. Technol.* 44 (13), 5270–5276. doi:10.1021/es903270w

Niu, B., Al-Menhali, A., and Krevor, S. C. (2015). The Impact of Reservoir Conditions on the Residual Trapping of Carbon Dioxide in B Erea Sandstone. *Water Resour. Res.* 51 (4), 2009–2029. doi:10.1002/2014wr016441

O'Connor, W. K., Dahlin, D. C., Nilsen, D. N., Walters, R. P., and Turner, P. C. (2000). *Carbon dioxide Sequestration by Direct Mineral Carbonation With Carbonic acid (No. DOE/ARC-2000-008).* Albany, OR: Albany Research Center (ARC).

Szeliski, R. (2010). *Computer Vision: Algorithms and Applications*. Springer Science and Business Media.

Vincent, L., and Soille, P. (1991). Watersheds in Digital Spaces: an Efficient Algorithm Based on Immersion Simulations. *IEEE Trans. Pattern Anal. Machine Intell.* 13, 583–598. doi:10.1109/34.87344

White, C. M., Smith, D. H., Jones, K. L., Goodman, A. L., Jikich, S. A., LaCount, R. B., et al. (2005). Sequestration of Carbon dioxide in Coal With Enhanced Coalbed Methane Recovery a Review. *Energy Fuels* 19 (3), 659–724.

Yu, H., Zhang, Y., Lebedev, M., Han, T., Verrall, M., Wang, Z., et al. (2018a). Nanoscale Geomechanical Properties of Western Australian Coal. *J. Pet. Sci. Eng.* 162, 736–746. doi:10.1016/j.petrol.2017.11.001

Yu, H., Zhang, Y., Lebedev, M., Wang, Z., Ma, J., Cui, Z., et al. (2018b). CO2 Saturated Brine Injected into Fractured Shale: An X-ray Micro-tomography *In-Situ* Analysis at Reservoir Conditions. *Energ. Proced.* 154, 125–130. doi:10.1016/j.egypro.2018.11.021

Yu, H., Zhang, Y., Lebedev, M., Wang, Z., Verrall, M., and Iglauer, S. (2018c). "Reactive Flow in Unconsolidated sandstone: Application to Carbon Geosequestration," in Proceeding of the Abu Dhabi International Petroleum Exhibition & Conference, 2018 November (Texas: OnePetro).

Yu, H., Zhang, Y., Ma, Y., Lebedev, M., Ahmed, S., Li, X., et al. (2019a). CO 2 - Saturated Brine Injection into Unconsolidated Sandstone: Implications for Carbon Geosequestration. *J. Geophys. Res. Solid Earth* 124 (11), 10823–10838. doi:10.1029/2018jb017100

Yu, H., Zhang, Y., Lebedev, M., Wang, Z., Li, X., Squelch, A., et al. (2019b). X-ray Micro-computed Tomography and Ultrasonic Velocity Analysis of Fractured Shale as a Function of Effective Stress. *Mar. Pet. Geology.* 110, 472–482. doi:10.1016/j.marpetgeo.2019.07.015

Yuan, Y., Rezaee, R., Yu, H., Zou, J., Liu, K., and Zhang, Y. (2021). Compositional Controls on Nanopore Structure in Different Shale Lithofacies: A Comparison with Pure Clays and Isolated Kerogens. *Fuel* 303, 121079. doi:10.1016/j.fuel.2021.121079

Zhang, Y., Lebedev, M., Sarmadivaleh, M., Barifcani, A., and Iglauer, S. (2016). Swelling-induced Changes in Coal Microstructure Due to Supercritical CO2injection. *Geophys. Res. Lett.* 43, 9077–9083. doi:10.1002/2016gl070654

Zhang, Y., Zhang, Z., Sarmadivaleh, M., Lebedev, M., Barifcani, A., Yu, H., and Iglauer, S. (2017). Micro-scale Fracturing Mechanisms in Coal Induced by Adsorption of Supercritical CO 2. *Int. J. Coal Geology.* 175, 40–50. doi:10.1016/j.coal.2017.04.002

Zhang, Y., Lebedev, M., Yu, H., and Iglauer, S. (2018). Experimental Study of Supercritical CO2 Injected into Water Saturated Medium Rank Coal by X-ray MicroCT. *Energ. Proced.* 154, 131–138. doi:10.1016/j.egypro.2018.11.022

Zhang, Y., Zhang, Z., Arif, M., Lebedev, M., Busch, A., Sarmadivaleh, M., et al. (2020). Carbonate Rock Mechanical Response to CO2 Flooding Evaluated by a Combined X-ray Computed Tomography - DEM Method. *J. Nat. Gas Sci. Eng.* 84, 103675. doi:10.1016/j.jngse.2020.103675

Zhou, Y., Hatzignatiou, D. G., and Helland, J. O. (2017). On the Estimation of CO 2 Capillary Entry Pressure: Implications on Geological CO 2 Storage. *Int. J. greenhouse gas Control* 63, 26–36. doi:10.1016/j.ijggc.2017.04.013

Conflict of Interest: The authors declare that the research was conducted in the absence of any commercial or financial relationships that could be construed as a potential conflict of interest.

The handling editor declared a past co-authorship with the author HY.

Publisher's Note: All claims expressed in this article are solely those of the authors and do not necessarily represent those of their affiliated organizations, or those of the publisher, the editors, and the reviewers. Any product that may be evaluated in this article, or claim that may be made by its manufacturer, is not guaranteed or endorsed by the publisher.